

This is the **Accepted Version** of a paper published in the journal *Water Science and Technology*:

Schneider, Philip A., Wallace, James W., and Tickle, Julian C. (2013) *Modelling and dynamic simulation of struvite precipitation from source-separated urine*. *Water Science and Technology*, 67 (12). pp. 2724-2732.

<http://dx.doi.org/10.2166/wst.2013.184>

# Modelling and Dynamic Simulation of Struvite Precipitation from Source Separated Urine

**Philip A. Schneider\*, James W. Wallace and Julian C. Tickle**

School of Engineering and Physical Sciences, James Cook University, Townsville, Queensland, 4811, Australia

\*Corresponding author (Phil.Schneider@jcu.edu.au)

## Abstract

A model of a mixed-mode nutrient recovery reactor is developed for a urine feed, incorporating complex solution thermodynamics, dynamic conservation relations and a power-law kinetic expression for crystal growth from seed crystals. Simulations at nominal operating conditions predict phosphorus recoveries greater than 99%, based on existing process kinetic parameters and operating conditions employed in previously published studies. The overall rate of nutrient recovery depends on Saturation Index of the precipitating solid, the available surface area for mass transfer and the feed rate of the limiting constituent ion. Under the conditions considered, the nutrient feed rate appears to be the limiting factor for precipitation. Simulations demonstrate that diurnal feed flow variations of  $\pm 50\%$  have a small effect on the rate of nutrient recovery. Overall, the study shows that valuable insights are gained in relation to process performance predictions, which should lead to more confident process design, operation and control.

## Keywords

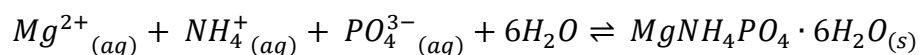
Nutrient removal and recovery, source-separated urine; struvite; process modelling; kinetics; thermodynamics.

## INTRODUCTION

Phosphorous is an essential nutrient for all living things. The human population consumes approximately 40 million tons of phosphate rock per year and, with annual demand increasing by 1.5%, it is estimated that approximately 100 years of phosphate rock reserves (Shu, Schneider, Jegatheesan, & Johnson, 2006). Therefore, alternative phosphorous sources are becoming increasingly important. Source-separated urine is one such potential feedstock (Etter, Tilley, Khadka, & Udert, 2011).

Crystallisation/precipitation is an established recovery technique giving high removal rates, effective process control and stability of the resultant mineral phosphate, such as struvite (magnesium ammonium phosphate) (Bhuiyan, Mavinic, & Beckie, 2008). Nutrient recovery from source-separated urine has the potential to provide benefit to low socio-economic communities, which is ideal for distributed treatment systems.

Struvite formation occurs when magnesium, phosphate and ammonia react, according to the following stoichiometry.



A key challenge in the development of nutrient removal and recovery process is to manage the risks associated with process design. Since risk is inversely proportional to knowledge, it follows that the more we know about a proposed design, the better we can manage risk, lowering costs and mitigating unintended process design failures.

## METHODS

The methodology in this study involved the development of a process model in the form of differential and algebraic equations (DAEs). The DAEs are then solved (*i.e.* simulated) for a given set of process parameters (vessel volume, rate parameter values, *etc.*) and operating conditions (feed

concentration and flow rate, acid/base flow rates, *etc.*). Owing to its complexity, the model must be solved numerically. Once the equations can be solved to an acceptable error tolerance, a range of scenarios is considered to determine cause-and-effect behaviour and performance of the system.

## Model Development

A mixed-mode reactor, shown in Figure 1, is considered wherein the nutrient-rich urine flows through the reactor (*i.e.* continuous mode) and the precipitated solid phase is retained (*i.e.* batch mode) and then periodically harvested. The model for this system describes the solution thermodynamics, used to predict the driving force for crystal precipitation/growth, the dynamic mass conservation of all elements present in the liquid and solid phases, and a dynamic population balance that describes changes in the crystal population (Randolph & Larson, 1988).

**Figure 1: Schematic diagram of mixed-mode nutrient recovery reactor**

### *Solution thermodynamics*

The solution within the nutrient recovery reactor can be fully specified with a series of algebraic relations. Solution *pH* is defined by

$$pH = -\log(a_{H^+})$$

where  $a_{H^+}$  represents the activity of the hydride ion in solution.

Urine consists of a number of elements, including magnesium, chlorine, sodium, nitrogen, phosphorous, potassium, sulphur and carbon, distributed across a range of species (see Table 1), and must be accounted for. All equilibria are represented by an algebraic equation of the form

$$K_{products} = \frac{\prod \alpha_{products}}{\prod \alpha_{reactants}}$$

where  $\alpha$  is the activity of the products and reactants involved in the equilibrium relation.

**Table 1: Chemical equilibria considered in this study**

Equilibria	$pK$ (25°C, $\mu = 0$ )	Reference
$Mg^{2+} + OH^- \rightleftharpoons MgOH^+$	$pK_{MgOH^+} = 2.56$	(Ali & Schneider, 2008)
$NH_3 + H^+ \rightleftharpoons NH_4^+$	$pK_{NH_4^+} = 9.25$	
$PO_4^{3-} + H^+ \rightleftharpoons HPO_4^{2-}$	$pK_{HPO_4^{2-}} = 12.35$	

Equilibria	$pK$ (25°C, $\mu = 0$ )	Reference
$HPO_4^{2-} + H^+ \rightleftharpoons H_2PO_4^-$	$pK_{H_2PO_4^-} = 7.20$	
$Mg^{2+} + H_2PO_4^- \rightleftharpoons MgH_2PO_4^+$	$pK_{MgH_2PO_4^+} = 1.51$	(Doyle & Parsons, 2002)
$CO_3^{2-} + H^+ \rightleftharpoons HCO_3^-$	$pK_{HCO_3^-} = 10.33$	(Ronteltap, Maurer, & Gujer, 2007)
$Mg^{2+} + HCO_3^- \rightleftharpoons MgHCO_3^+$	$pK_{MgHCO_3^+} = 1.07$	
$Mg^{2+} + HCO_3^- \rightleftharpoons MgCO_3 (aq) + H^+$	$pK_{MgCO_3} = -7.35$	
$Na^+ + H_2PO_4^- \rightleftharpoons NaHPO_4^- + H^+$	$pK_{NaHPO_4^-} = -6.01$	
$NH_4^+ + H_2PO_4^- \rightleftharpoons NH_4HPO_4^-$	$pK_{NH_4HPO_4^-} = 1.30$	
$Mg^{2+} + H_2PO_4^- \rightleftharpoons MgPO_4^- + 2H^+$	$pK_{MgPO_4^-} = -12.96$	
$Mg^{2+} + H_2PO_4^- \rightleftharpoons MgHPO_4 + H^+$	$pK_{MgHPO_4} = -4.30$	
$H^+ + OH^- \rightleftharpoons H_2O$	$pK_{H_2O} = -7$	(Stumm & Morgan, 1996)
$HCO_3^- + H^+ \rightleftharpoons H_2CO_3 (aq)$	$pK_{H_2CO_3} = 6.35$	(K.M. Udert, Larsen, & Gujer, 2003)
$Na^+ + HCO_3^- \rightleftharpoons NaHCO_3 (aq)$	$pK_{NaHCO_3} = -0.25$	
$Na^+ + CO_3^{2-} \rightleftharpoons NaCO_3^-$	$pK_{NaCO_3^-} = 1.27$	
$Na^+ + H_2PO_4^- \rightleftharpoons NaH_2PO_4 (aq)$	$pK_{NaH_2PO_4} = 0.25$	
$2Na^+ + H_2PO_4^- \rightleftharpoons Na_2HPO_4 (aq) + H^+$	$pK_{Na_2HPO_4} = -6.11$	
$NH_4^+ + H_2PO_4^- \rightleftharpoons NH_4H_2PO_4 (aq)$	$pK_{NH_4H_2PO_4} = 0.10$	
$K^+ + H_2PO_4^- \rightleftharpoons KH_2PO_4 (aq)$	$pK_{KH_2PO_4} = 0.23$	
$K^+ + H_2PO_4^- \rightleftharpoons KHPO_4^- + H^+$	$pK_{KHPO_4^-} = -6.12$	
$K^+ + SO_4^{2-} \rightleftharpoons KSO_4^-$	$pK_{KSO_4^-} = 0.85$	
$Mg^{2+} + SO_4^{2-} \rightleftharpoons MgSO_4 (aq)$	$pK_{MgSO_4} = 2.37$	
$Na^+ + SO_4^{2-} \rightleftharpoons NaSO_4^-$	$pK_{NaSO_4^-} = 0.70$	
$NH_4^+ + SO_4^{2-} \rightleftharpoons NH_4SO_4^-$	$pK_{NH_4SO_4^-} = 1.03$	

Solution  $pH$  is determined by the inclusion of the electroneutrality condition (*i.e.* charge balance), which is

$$\sum_{i=1}^n C_i Z_i = 0$$

where  $C_i$  is the analytic concentration of ionic species,  $i$ , and  $Z_i$  its charge, either  $Z_1 = \pm 1$ ,  $Z_2 = \pm 2$  or  $Z_3 = \pm 3$ .

Owing to real solution effects, the activity of each ion,  $i$ , is employed instead of its concentration

$$a_i = \gamma_i C_i$$

where  $\gamma_i$  is the activity coefficient for the species in question and takes a value of either  $\gamma_1$ ,  $\gamma_2$  or  $\gamma_3$ , depending on its charge. Owing to the high ionic strength of urine,  $\gamma_i$  values were based on the Debye-Hückel equation (Ronteltap et al., 2007) with Davies approximation

$$\log(\gamma_i) = A Z_i^2 \left( \frac{\sqrt{\mu}}{1 + \sqrt{\mu}} - 0.3\mu \right)$$

where A is a temperature-dependent constant ( $A = 0.509$  at  $25^\circ\text{C}$ ) and  $\mu$  is the ionic strength of the solution, given by

$$\mu = \frac{1}{2} \sum_{i=1}^m C_i Z_i^2$$

A key thermodynamic variable is the saturation index, or  $SI$ , which, for struvite, is

$$SI = \log \left( \frac{(a_{Mg^{2+}}) (a_{PO_4^{3-}}) (a_{NH_4^+})}{K_{sp}} \right)$$

where  $K_{sp}$  is the equilibrium solubility product of struvite, and the numerator is the ion activity product of struvite's constituent ions. The numeric value of  $SI$  determines its thermodynamic state: positive, the solution is supersaturated in struvite; negative, the solution is undersaturated; and zero, saturated. The  $SI$  of solution will be used as the driving force for the molar precipitation rate of struvite.

#### Conservation of elements

The total liquid-phase concentration for each element,  $C_j^{tot}$ , is the sum of concentration of those complexes,  $i$ , that contain element  $j$ , taking into account the stoichiometric proportion of the element  $j$  in complex  $i$ ,  $\nu_{j,i}$ .

$$C_j^{tot} = \sum_{i=1}^n \nu_{j,i} C_i$$

Each of the seven elements in the system must be conserved. The following differential equation describes each element's molar inventory in a well-mixed solution.

$$\frac{d(C_j^{tot})}{dt} V + \frac{d(V)}{dt} C_j^{tot} = C_j^{in} F_{in} - C_j^{tot} F_{out} - \nu_{j, struvite} Rate_{struvite}$$

In the above relation  $V$  is the liquid volume in the reactor,  $F_{in}$  and  $F_{out}$ , are the flows (in and out) of the reactor and  $C_j^{in}$  is the concentration of element  $j$  in the combined feed stream. The far right hand term accounts for the rate loss of elements from liquid to solid phase, where  $Rate_{struvite}$  is the molar formation rate of struvite and  $\nu_{j, struvite}$  is the stoichiometric proportion of the elements found in struvite (*i.e.* magnesium, nitrogen or phosphorus).

The liquid volume in the reactor is subject to change, depending on the in and out flows, and will be reduced as the volume of retained precipitant typically increases.

$$\frac{dV}{dt} = F_{in} - F_{out} - \frac{dV_{struvite}}{dt}$$

### Struvite formation rate

While previous workers (Nelson, Mikkelsen, & Hesterberg, 2003; Quintana et al., 2005; Turker & Celen, 2007) modelled the rate of desupersaturation of the solution, the approach taken in this work considers the formation rate of solid struvite. This rate depends on characteristics of the particles, such as their number, geometry and the thermodynamic state of the solution.

While struvite crystals/particles are clearly non-spherical, it is convenient to track the number-average diameter of spheres of the same volume as the struvite crystal in question. As such, the variable  $\bar{L}$  is the average spherical-volume-equivalent diameter, which can be used to determine the volume of the crystal

$$v = \frac{\pi}{6} \bar{L}^3$$

and thus its rate of change with time is

$$\frac{dv}{dt} = \frac{\pi}{6} 3\bar{L}^2 \frac{d\bar{L}}{dt}$$

The rate of change of the spherical volume-equivalent diameter of a struvite crystal,  $\bar{L}$ , is assumed to have a power-law dependency on the saturation index,  $SI$ , of struvite.

$$\frac{d\bar{L}}{dt} = kSI^n$$

The power law dependency (*i.e.*  $n$ ) is expected to lie between 1<sup>st</sup> to 2<sup>nd</sup> order (Bouropoulos & Koutsoukos, 2000; Kofina & Koutsoukos, 2005), while the rate coefficient,  $k$ , must be determined by experiment (Ali & Schneider, 2008). This approach is similar to that of (Bhuiyan et al., 2008), except that it does not include a diffusion effect in the growth model, since the system is well mixed and therefore diffusion effects are not considered important.

The rate of change of the total volume of crystal present requires knowledge of the total number of crystals present,  $N_{struvite}$ , which is assumed to be constant, implying that no nucleation takes place. Clearly this is not the case, but was assumed to radically simplify the problem.

$$\frac{dV_{struvite}}{dt} = N_{struvite} \frac{dv}{dt}$$

It follows that the molar rate of change of struvite,  $Rate_{struvite}$ , is

$$Rate_{struvite} = \frac{\rho_{struvite}}{MW_{struvite}} \frac{dV_{struvite}}{dt}$$

where the density of the crystal is represented by  $\rho_{struvite}$  and the molecular weight of struvite is  $MW_{struvite}$ .

The recovery of phosphorus is a key performance measure of any nutrient recovery system. Its recovery is based on the thermodynamic efficiency, which accepts the fact that not all of the phosphorus can be removed (since it remains, unattainable, in the saturated solution). As such, phosphorus recovery was defined as

$$\% Recovery = \frac{(C_j^{in} F_{in} - C_j^{tot} F_{out})}{(C_j^{in} F_{in} - C_j^{sat} F_{out})} 100\%$$

where  $C_j^{sat}$  is the elemental concentration of the feed solution in its saturated state.

## Simulation

With appropriate initial conditions for the differential equations, inlet flows and concentrations, and kinetic and operational parameter values, the set of DAEs was solved using Engineering Equation Solver<sup>1</sup> (EES), predicting the time-varying (*i.e.* dynamic) behaviour of the system.

### *Initial conditions and process specifications*

Table 2 specifies the reactor initial conditions, feed compositions and flows and reactor specifications. The liquid phase initial conditions was specified to be urine, saturated in struvite. A 1-litre reactor volume was chosen as a matter of convenience, and could be scaled to larger volumes (assuming that the system remains well mixed with increasing size). It was arbitrarily decided that the system would operate on a repeating 10-day cycle, at which time the system is allowed to equilibrate and then the accumulated struvite is harvested, returning the system to its initial conditions. The urine feed was modelled as though the compounds listed in the same table had been blended and the urea was fully hydrolysed. The nominal flow and concentration of the urine, magnesium source and sodium hydroxide streams are also detailed. The hydraulic retention time of 10 hours is similar to the system operated by Ronteltap (Ronteltap, Maurer, Hausherr, & Gujer, 2010). The feed condition was formulated such that the molar supply rate of magnesium was equivalent to that of phosphorus.

**Table 2: Initial conditions, reactor specifications, feed compositions and flows to the reactor**

Initial Liquid Elemental Composition		Initial Solids		Reactor Specifications	
<i>Mg</i>	0.2768 mM	$L_i$	$50 \times 10^{-6} \text{ m}$	$V$	1 L
<i>Cl</i>	185.9 mM	$m_i$	20g	$t_{final}$	10 days
<i>Na</i>	91.11 mM	<b>Recipe for synthetic feed urine</b>			
<i>N</i>	501.4 mM	$Na_2SO_4$	16.0 mM	$NaCl$	51.0 mM
<i>P</i>	0.2768 mM	$KCl$	46.0 mM	$NH_4HCO_3$	266.0 mM
<i>K</i>	41.91 mM	$NH_4Cl$	73.0 mM	$NH_3$	228.0 mM
<i>S</i>	14.58 mM	$NaH_2PO_4$	17.0 mM		
<i>C</i>	242.3 mM	<b>Other feed stream compositions and flows</b>			
		<i>urine</i>	As above.		0.1 L/h
		$MgCl_2$	170 mM		0.01 L/h
		$NaOH$	100 mM		0.000 L/h

### *Thermodynamic and kinetic parameters*

The  $pK$  values, given in Table 1, define the chemical equilibria.

The solubility product for struvite was  $pK_{sp} = -13.26$  (Ohlinger, Young, & Schroeder, 1998). Of course other values could be used to assess the importance of this parameter.

<sup>1</sup> F-Chart Software, Box 44042, Madison, WI 53744

The kinetic parameters chosen for the crystal growth rate expression were reported earlier (Ali & Schneider, 2008). The rate coefficient was  $k = 1 \times 10^{-6} \text{ m/h}$ , and the order of the linear growth rate was  $n = 1.5$ .

The set of DAEs was composed of 252 equations, 12 of which were differential and 240 algebraic. EES, as with any numeric solver, requires valid initial guesses (not to be confused with initial conditions for the differential equations!) for all unknown variables. As such, the EES input file must be interactively *built*, updating these guess values along the way.

The EES input file was formulated so that the system was fed a constant flow of urine and  $\text{MgCl}_2$  solutions. An EES procedure was created such that both inlet flows changed to zero once the process had completed 90% of the 10-*day* (240 *h*) operational cycle or campaign. This was done to simulate the exhaustion of struvite from solution, after which the solid struvite material is harvested. This leaves a saturated solution, ready to be seeded with solid struvite for the next operational cycle.

## RESULTS AND DISCUSSION

### Results

Owing to the release of ammonium by urea hydrolysis, the urine feed solution *pH* was calculated by the model to have an equilibrium value of *pH* = 9.0. This was encouraging, since other workers observed similar behaviour for real urine (Ronteltap et al., 2007; K. M. Udert, Larsen, Biebow, & Gujer, 2003). As a result, no sodium hydroxide was required to generate a positive *SI*, and, thus, its flow was set to zero in all simulations.

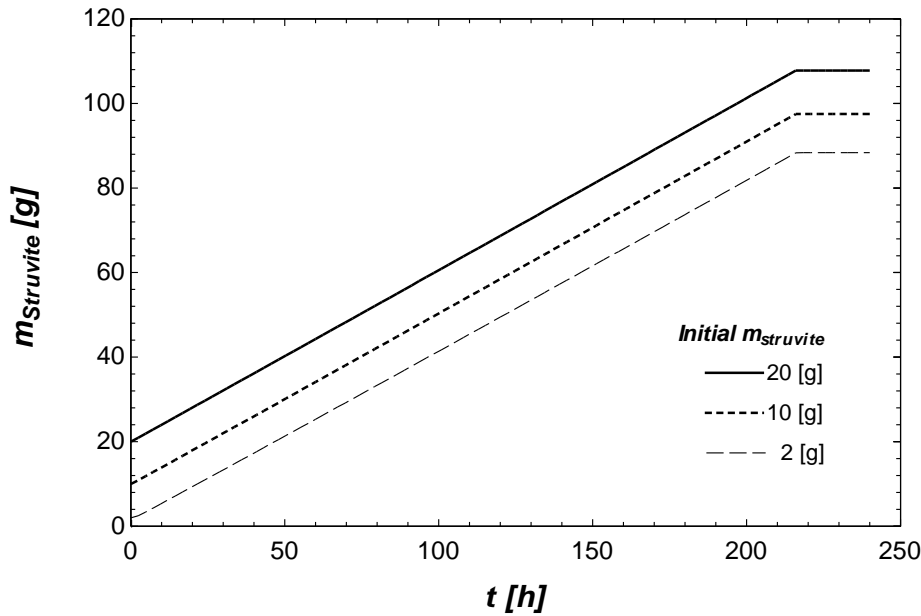
The formation, and subsequent retention, of struvite in the reactor are shown in Figure 2 for a range of initial seed mass,  $m_i$  (2*g*, 10*g* and 20*g*). All cases show strikingly similar rates of struvite accumulation, as seen by the parallel slopes, despite the tenfold range in the initial mass. This suggests that  $m_i = 2\text{g}$  offers adequate surface area (*i.e.* buffering) to accommodate the necessary mass transfer.

During the last 10% of the campaign, when the urine and magnesium inlet flows were set to zero, it is interesting to note that solution desupersaturation offers very little additional increase in struvite mass, illustrating the highly non-linear (and highly sensitive) dependency of changes in the saturation index to changes in the solution mass balance.

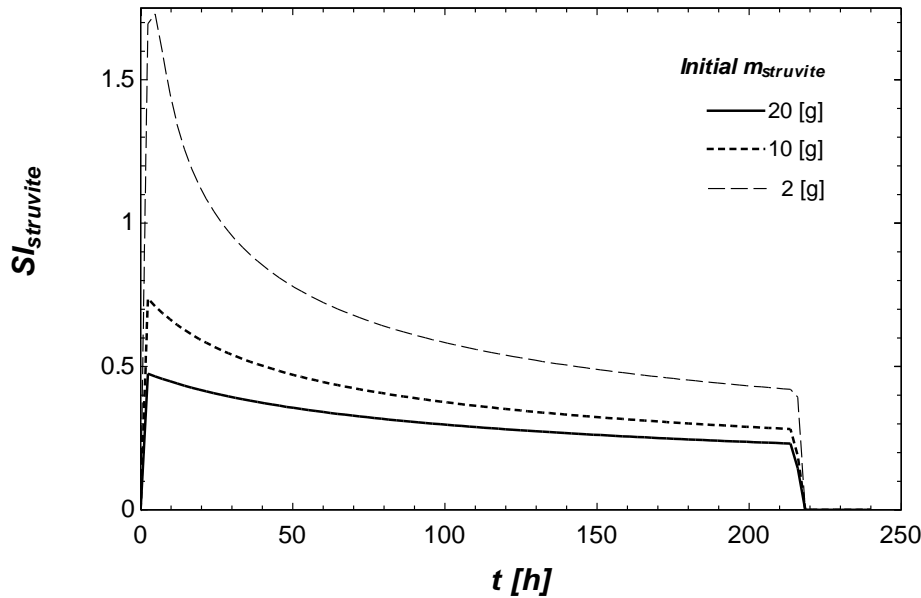
Figure 3 shows the temporal trajectories of struvite *SI*, again for the same range of starting seed quantities. At the start of each cycle, the *SI* = 0, owing to the use of the saturated urine from the previous cycle. However, *SI* rises rapidly upon commencement of urine and magnesium feeding, then declines slowly throughout the remainder of the operational campaign. It is of interest to note that larger values for  $m_i$  lead to reduced struvite *SI* peaks. This is due to the larger initial, and subsequent, surface area for mass transfer, which requires a lower thermodynamic driving force for the same recovery rate. This is an extremely important feature and suggests that retaining more solids should lead to enhanced nutrient recoveries.

Figure 3 also shows that on day 9, when the urine feed is turned off, the struvite *SI* drops sharply to zero, indicating that the solution becomes saturated and that no further struvite can be recovered. It also shows that much less than 10% of the period of the campaign is required for desupersaturation, which shows the predictive capability of the model to the specification of a process design and its operation.



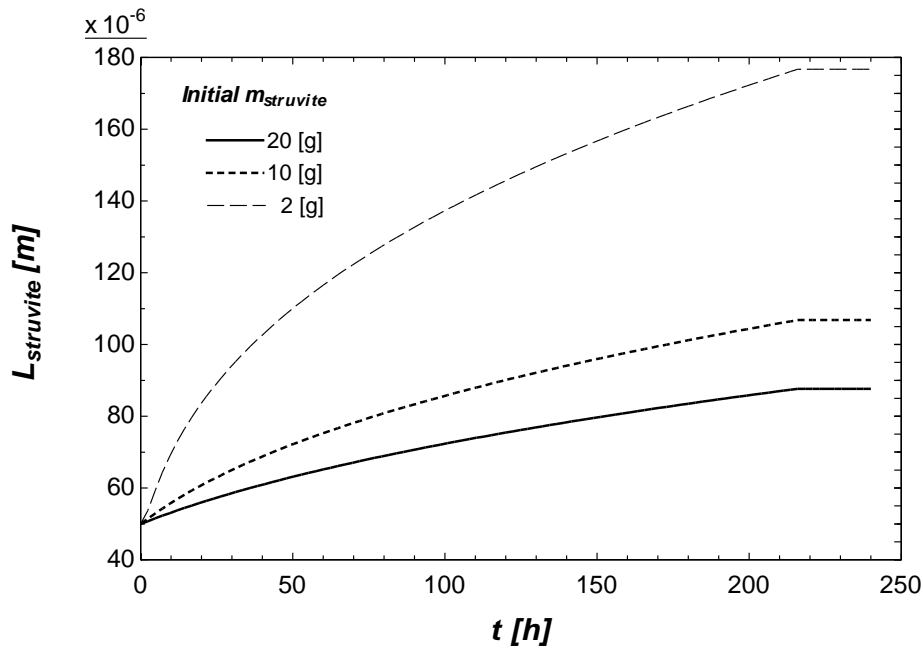


**Figure 2: Mass of struvite produced and retained in 10-day operation of nutrient recovery reactor with varying initial amounts of struvite**



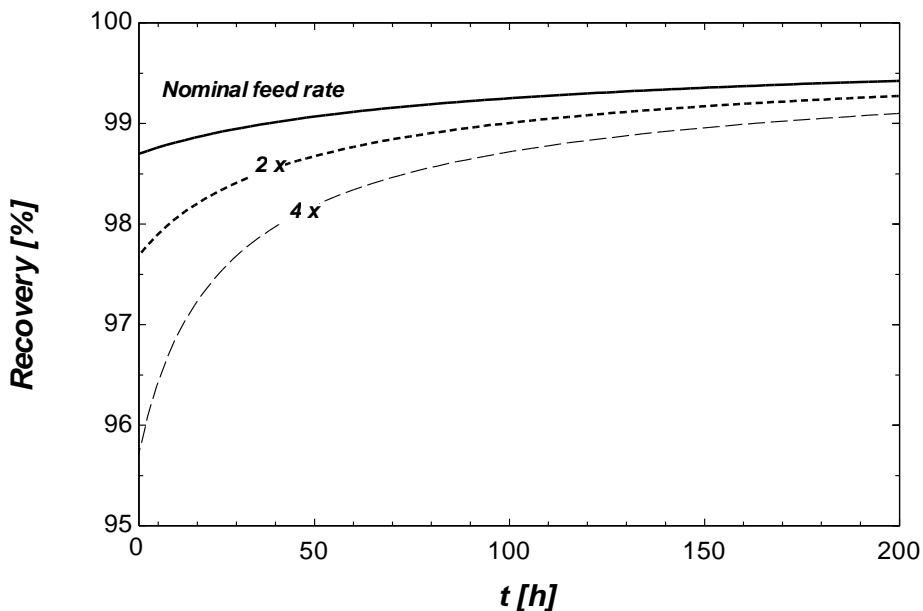
**Figure 3: Struvite saturation index in 10-day operation of nutrient recovery reactor with varying initial amounts of struvite**

Figure 4 shows the effect of the initial mass of struvite on the average crystal size,  $\bar{L}$ , throughout the operating time. As expected, the greatest mass of initial struvite, and thus the greatest number of crystals,  $N_{struvite}$ , requires these crystals grow less than the cases where less initial struvite mass is present. This corresponds directly to the lower  $SI$  profile in Figure 3, since less thermodynamic driving force is required to grow the crystals to a smaller ultimate size.



**Figure 4: Length of struvite crystals in 10-day operation of nutrient recovery reactor with varying initial amounts of struvite**

At the nominal feed rate of urine, phosphorus recovery quickly rises to better than 98.5% and over the 10-day campaign approaches 99.5%, as pictured in Figure 5. At double and quadruple rates of urine feed, recovery approaches lower ultimate values. This again shows the predictive capability of the model in relation to process design and operation, suggesting that a number of scenarios could be played out *before* construction and operation of such a unit is executed. Clearly this reduces the risk of uncertainties affecting health and safety, financial and/or operational matters.



**Figure 5: Phosphorus recovery in 10-day operation of nutrient recovery reactor with varying feed rates**

Consideration is also given to the operational impact of a diurnal variation in the urine feed rate with an amplitude of  $\pm 50\%$  around its nominal rate of flow. The resultant *SI* trajectories are very sensitive to these feed rate variations, as shown in Figure 6, and it is clear that operation with a lower mass of struvite is more sensitive.

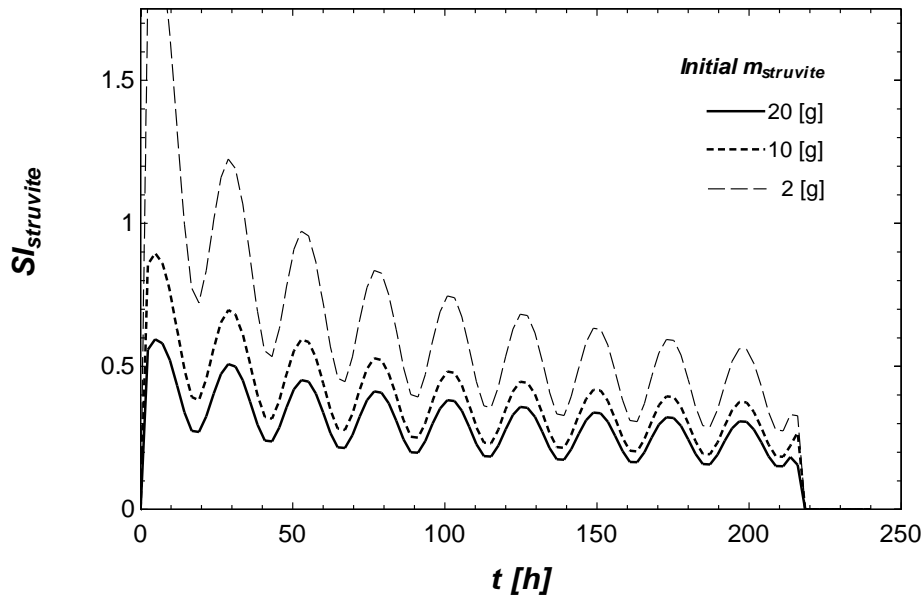


**Figure 6: Struvite saturation index in 10-day operation of nutrient recovery reactor with varying initial amounts of struvite subjected to a sinusoidal variation in urine feed**

Interestingly, the struvite mass trajectories are much less sensitive to these flow variations, as shown in Figure 7, and show that the same quantity of struvite is recovered, as before. This is due to the fact that the struvite mass results from the integral of the flow, which attenuates the impact of these very significant feed variations.

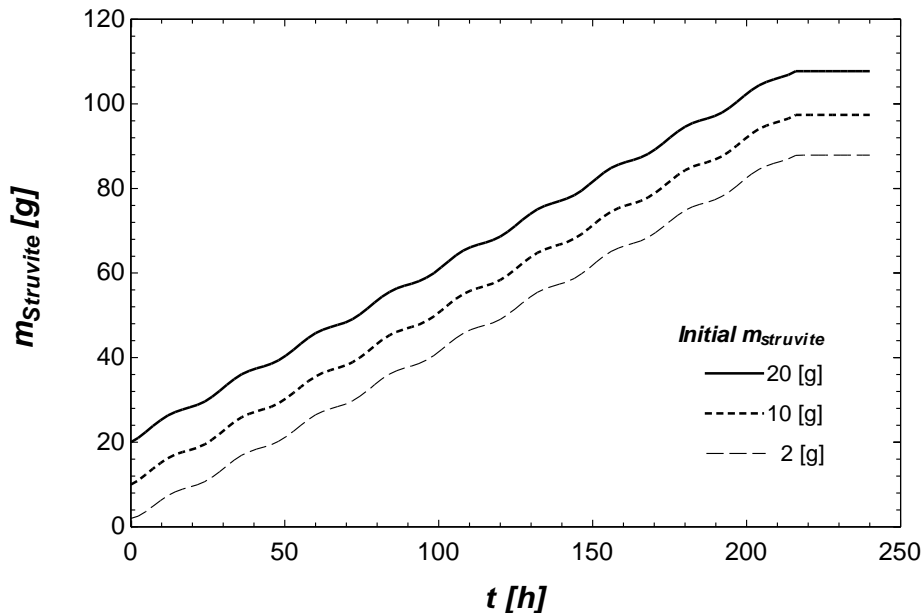


**Figure 7: Mass of struvite produced and retained in 10-day operation of nutrient recovery reactor with varying initial amounts of struvite subjected to a sinusoidal variation in urine feed**

## Discussion

Why does the mass deposition rate of struvite appear to be insensitive to the initial mass of seed struvite employed? In answer to this it is important to recognise that while a positive  $SI$  is a necessary condition of struvite supersaturation, this alone is not sufficient to predict the rate of struvite recovery. Rather, it is the combination of the  $SI$ , along with the surface area available for mass transfer, that determines the overall mass deposition rate of struvite ion constituents. As shown in Figure 3, if less seed crystal is employed, the available surface area is reduced, limiting

the mass deposition rate of struvite, in turn leading to higher levels of *SI* in the reactor. In the extreme case, the system would be so limited by the lack of surface area that the *SI* would build to extremely high levels that would lead to excessive nucleation of struvite, rather than seed crystal growth.

The rapid and significant decline in struvite *SI* during the last day of operation is also of interest, since it was put in place to offer a final exhaustion of struvite from the solution. Counterintuitively, the large drop (*i.e.* 0.25) in the *SI* at the end of the cycle (see Figure 3) yields only a slight additional recovery of struvite, as shown in Figure 2. To explain this reference is made to Figure 8, which shows the log-concentration of the struvite constituent ions (*i.e.*  $NH_4^+$ ,  $Mg^{2+}$  and  $PO_4^{3-}$ ) over the duration of the campaign. Clearly, the final drop in *SI* occurs due in large part to the reduction in the concentrations of  $Mg^{2+}$  and  $PO_4^{3-}$  ions. However, at such low concentrations, this reduction in *SI* causes only a small change in the mass balance of the system (in the order to  $10^{-4}$  molar). This implies that there is a significant nonlinear element to the system's thermodynamic behaviour and, as such, caution should be exercised when using *SI* as the driving force for the rate of precipitation without careful consideration of these nonlinearities.

Figure 8 also shows that the non-equilibrium solution species ratios ( $NH_4^+ : Mg^{2+} : PO_4^{3-}$ ) of approximately ( $10^{-1} : 10^{-4} : 10^{-7}$ ), even though the magnesium and phosphorus inlet flows were equimolar. This occurs because the  $PO_4^{3-}$  tends to complex with a wider range of ions, leaving less free phosphate available for struvite formation. Thus it is the release rate of  $PO_4^{3-}$  into the solution, and not simply the feed rate of total phosphorus in urine, that determines the *SI* and thus the recovery rate of struvite. This underlines the importance of modelling solution thermodynamics in nutrient recovery systems.

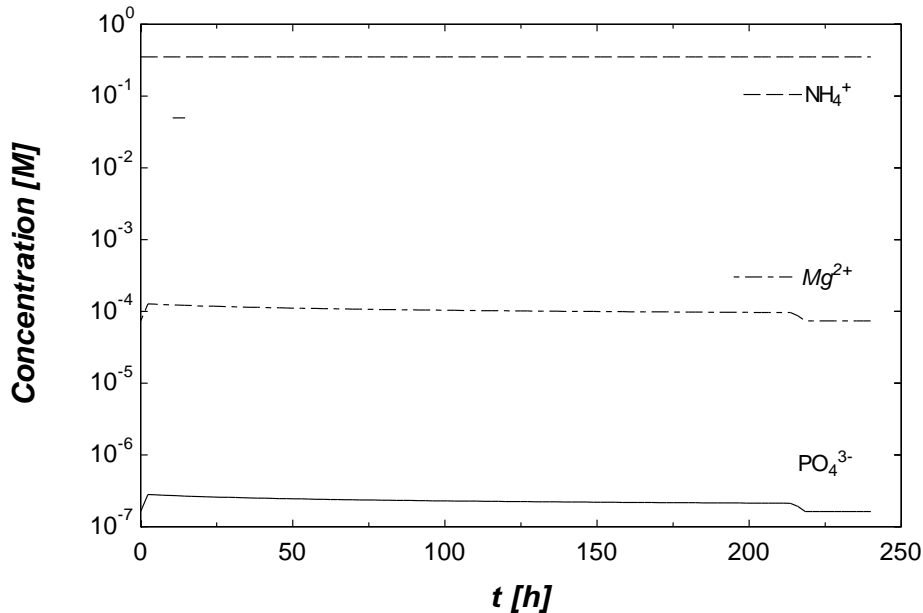


**Figure 8: Struvite constituent ion concentrations in 10-day operation of nutrient recovery reactor at nominal operating conditions**

It is also apparent that the process is self regulating in the face of significant variations in urine feed rates, which is due to the buffering effect of the surface area available for struvite deposition. This implies that limited process control would likely be required to maintain reasonably stable nutrient recovery rates, as long as a sufficient level of seed crystal is employed.

## CONCLUSIONS

The model that was developed to describe the dynamic behaviour of a mixed-mode nutrient recovery reactor predicted the recovery rate of struvite from a hydrolysed urine feed. The set of DAEs were successfully simulated across a range of operating conditions.

Recovery of phosphorus appears to be better than 99% across the range of hydraulic residence times considered.

Recovery rates of struvite from a urine feed are insensitive to variations mass of struvite seed present in the range investigated, but instead depended on the rate of feed of the limiting nutrient. Dynamic feed flow variations of  $\pm 50\%$  were attenuated in terms of their impact on the rate of recovery of nutrients from the feed.

Significant insights into process design and operation result from the modelling and simulation of such systems, and should be incorporated into the design of any nutrient recovery system.

## REFERENCES

- Ali, M. I., & Schneider, P. A. (2008). An approach of estimating struvite growth kinetic incorporating thermodynamic and solution chemistry, kinetic and process description. *Chemical Engineering Science*, 63(13), 3514-3525. doi: DOI: 10.1016/j.ces.2008.04.023
- Bhuiyan, M. I. H., Mavinic, D. S., & Beckie, R. D. (2008). Nucleation and growth kinetics of struvite in a fluidized bed reactor. *Journal of Crystal Growth*, 310(6), 1187-1194. doi: DOI: 10.1016/j.jcrysgro.2007.12.054
- Bouropoulos, N. C., & Koutsoukos, P. G. (2000). Spontaneous precipitation of struvite from aqueous solutions. *Journal of Crystal Growth*, 213(3-4), 381-388.
- Doyle, J. D., & Parsons, S. A. (2002). Struvite formation, control and recovery. *Water Research*, 36(16), 3925-3940. doi: Doi: 10.1016/s0043-1354(02)00126-4
- Etter, B., Tilley, E., Khadka, R., & Udert, K. M. (2011). Low-cost struvite production using source-separated urine in Nepal. *Water Research*, 45(2), 852-862. doi: DOI: 10.1016/j.watres.2010.10.007
- Kofina, A. N., & Koutsoukos, P. G. (2005). Spontaneous precipitation of struvite from synthetic wastewater solutions. *Crystal Growth & Design*, 5(2), 489-496.
- Nelson, N. O., Mikkelsen, R. L., & Hesterberg, D. L. (2003). Struvite precipitation in anaerobic swine lagoon liquid: effect of pH and Mg : P ratio and determination of rate constant. *Bioresource Technology*, 89(3), 229-236. doi: 10.1016/S0960-8524(03)00076-2
- Ohlinger, K. N., Young, T. M., & Schroeder, E. D. (1998). Predicting struvite formation in digestion. *Water Research*, 32(12), 3607-3614.
- Quintana, M., Sanchez, E., Colmenarejo, M. F., Barrera, J., Garcia, G., & Borja, R. (2005). Kinetics of phosphorus removal and struvite formation by the utilization of by-product of magnesium oxide production. *Chemical Engineering Journal*, 111(1), 45-52. doi: 10.1016/j.cej.2005.05.005

- Randolph, A. D., & Larson, M. A. (1988). *Theory of particulate processes : analysis and techniques of continuous crystallization* (2nd ed.). San Diego: Academic Press.
- Ronteltap, M., Maurer, M., & Gujer, W. (2007). Struvite precipitation thermodynamics in source-separated urine. *Water Research*, *41*(5), 977-984. doi: 10.1016/j.watres.2006.11.046
- Ronteltap, M., Maurer, M., Hausherr, R., & Gujer, W. (2010). Struvite precipitation from urine - Influencing factors on particle size. *Water Research*, *44*(6), 2038-2046. doi: 10.1016/j.watres.2009.12.015
- Shu, L., Schneider, P., Jegatheesan, V., & Johnson, J. (2006). An economic evaluation of phosphorus recovery as struvite from digester supernatant. *Bioresource Technology*, *97*(17), 2211-2216. doi: DOI 10.1016/j.biortech.2005.11.005
- Stumm, W., & Morgan, J. J. (1996). *Aquatic Chemistry* (3rd ed.). New York: Wiley.
- Turker, M., & Celen, I. (2007). Removal of ammonia as struvite from anaerobic digester effluents and recycling of magnesium and phosphate. *Bioresource Technology*, *98*(8), 1529-1534. doi: 10.1016/j.biortech.2006.06.026
- Udert, K. M., Larsen, T. A., Biebow, M., & Gujer, W. (2003). Urea hydrolysis and precipitation dynamics in a urine-collecting system. *Water Research*, *37*(11), 2571-2582. doi: 10.1016/S0043-1354(03)00065-4
- Udert, K. M., Larsen, T. A., & Gujer, W. (2003). Estimating the precipitation potential in urine-collecting systems. *Water Research*, *37*(11), 2667-2677.